Saudi Pharmaceutical Journal 30 (2022) 815–824

Contents lists available at ScienceDirect

Saudi Pharmaceutical Journal

journal homepage: www.sciencedirect.com

Original article

Determination of anticancer potential of a novel pharmacologically active thiosemicarbazone derivative against colorectal cancer cell lines

Azmat Ali Khan [a,*], Rehan Ahmad [b,*], Amer M. Alanazi [a], Nawaf Alsaif [a], Maha Abdullah [b], Tanveer A. Wani [a], Mashooq A. Bhat [a]

[a] Pharmaceutical Biotechnology Laboratory, Department of Pharmaceutical Chemistry, College of Pharmacy, King Saud University, Riyadh 11451, P.O. Box 2457, Saudi Arabia
[b] Colorectal Research Chair, Department of Surgery, College of Medicine, King Saud University, Riyadh 11451, P.O. Box 2457, Saudi Arabia.

ARTICLE INFO

Article history:
Received 13 December 2021
Accepted 18 March 2022
Available online 31 March 2022

Keywords:
Thiosemicarbazone derivative
Anticancer agent
Colon cancer
Apoptosis
HT-29
SW620

ABSTRACT

Thiosemicarbazones have received noteworthy attention due to their numerous pharmacological activities. Various thiosemicarbazone derivatives have been reported to play a key role as potential chemotherapeutic agents for the management of cancer. Herein, we aimed to establish the anticancer efficacy of novel thiosemicarbazone derivative C4 against colon cancer *in vitro*. The MTT viability assay identified C4 as a promising anticancer compound in a panel of cancer cell lines with the most potent activity against colon cancer cells. Further, anticancer potential of C4 was evaluated against HT-29 and SW620 colon cancer cell lines considering the factors like cell adhesion and migration, oxidative stress, cell cycle arrest, and apoptosis. Our results showed that C4 significantly inhibited the migration and adhesion of colon cancer cells. C4 significantly increased the intracellular reactive oxygen species (ROS) and induced apoptotic cell death. Cell cycle analysis revealed that C4 interfered in the cell cycle distribution and arrested the cells at the G2/M phase of the cell cycle. Consistent with these results C4 also down-regulated the Bcl-XL and Bcl-2 and up-regulated the caspase-3 expression. These findings introduced C4 as the potential anticancer agent against colon cancer.

1. Introduction

Colon cancer is one of the life-threatening diseases in the world and is ranked as the third most common malignancy with an estimated 1096.6 million new cases diagnosed in 2018 (Ferlay et al., 2019). Colon cancer shows an incidence rate of 8.5% among all cancers and the five-year survival rate for patients with non-localized tumors is 11% (Jemal et al., 2009; Jung et al., 2007). In Saudi Arabia, of all the types of cancers diagnosed in 2011, colon cancer is categorized as the first one among males and the third among females (Saudi Moh, 2013). Incidences of colon cancer are closely associated with genetic and environmental factors, where the role and inhibition of oncogenes on the one hand and alcohol consumption, smoking, lifestyle, obesity, etc. on the other have been implicated in its pathogenesis (Jung et al., 2007). Due to its high incidence and mortality, it has become a clinically notable malignant disease. Among the various therapeutic options, surgical resection is the most preferred and effective choice (Giuliani et al., 2010). Depending on the type of metastatic growth and prevention of its reoccurrence, chemotherapy along with surgery is also suggested (Giacchetti et al., 1999). However, high toxicity and serious side effects limit the therapeutic efficacy of chemotherapeutic agents (Boursi and Arber, 2007; Lee and Park, 2003). In the last few years new preventive and therapeutic options are being explored to fight this fatal malignancy.

Thiosemicarbazones (TSC) are one of the promising candidates in drug designing because of their diverse range of biological activities. Their ability of chelating transition metals has urged investigations concerning catalysis and medicinal applications (Dong et al., 2018; Yang and Liang, 2018). A wide variety of TSCs and their derivatives are reported to possess antiviral, antifungal, and antibacterial properties depending on the parent aldehyde or ketone (Linciano et al., 2018; Montazeri et al., 2019; Nejabatdoust et al., 2019; Montazeri et al., 2020). In recent times, they have received considerable attention due to their anti-

* Corresponding authors.
E-mail addresses: azkhan@ksu.edu.sa (A.A. Khan), arehan@ksu.edu.sa (R. Ahmad).
Peer review under responsibility of King Saud University.

Production and hosting by Elsevier

https://doi.org/10.1016/j.jsps.2022.03.011
1319-0164/

proliferative activity and have been recognized as promising anticancer agents (Pape et al., 2016; Wang et al., 2017; Yee et al., 2017). Presently, TSC and its derivatives are being widely investigated in some Phase I and Phase II clinical trials against several types of cancers (Murren et al., 2003; Karp et al., 2008; Ma et al., 2008). Studies have shown that they exert their anticancer properties through various biological activities like chelation of metal ions, generation of reactive oxygen species (ROS), inhibition of ribonuclease reductase, inhibition of cell cycle, and modulation of cellular signaling pathways regulating cell proliferation and death (Richardson et al., 2009; Qi et al., 2018).

The fact that TSCs exhibit antitumor activities has compelled numerous researchers to synthesize and design novel anticancer agents. Investigators have synthesized many TSC derivatives with potential anticarcinogenic properties. Triapine or 3-AP (3-amino pyridine-2-carboxaldehyde) is among the first of the TSC derivatives with an anticancer activity that has entered the phase II clinical trials (Finch et al., 2000). The alterations at the phenolic groups or substitutions like phenoxy, methoxy, nitro, etc. at thioamide nitrogen atoms have resulted in the discovery of some interesting anticancer derivatives. These structurally modified derivatives have shown significant anticancer properties against various cell lines (Bejarbaneh et al., 2020; Lukmantara et al., 2013; Pingaew et al., 2013; Habibi et al., 2020; Habibzadeh et al., 2020; Jarestan et al., 2020). A group of derivatives from heterocyclic TSCs have shown antitumor activities due to their ability to inhibit ribonuclease reductase (Silva et al., 2017; Yousef et al., 2011). The prospective anticancer ability of TSCs, thereby, has led to the growing curiosity about synthesizing structurally modified TSC derivatives for improving the cellular pharmaceutical effects of existing or novel drugs.

Although a great deal of attention has been paid to the versatility of TSCs in the chelation of metal ions, we focused on the synthesis and anticancer evaluation of a new series of TSCs bearing cyclohexyl moiety. The previous studies from our laboratory have reported the successful synthesis of TSC compounds and their potential inhibitory effects on breast cancer cell lines (Bhat et al., 2015a,b). From this series, C2 (2-cyclohexyl-N-[(Z)-(3-methoxyphe nyl) methylidene]hydrazinecarbothioamide) and C10 (2-cyclo hexyl-N-[(Z)-(3-hydroxyphenyl)-methylidene]hydrazinecarbo thioamide) were further selected for the synthesis of new series of compounds. These TSC derivatives had 3-hydroxy/3-methoxy phenyl on one side and different groups at the terminal nitrogen. The compounds have already been characterized analytically, spectrally, and physicochemically. They have also exhibited potential anticancer activity on SKBr-3 and BT-474 breast cancer cell lines (Bhat et al., 2015a,b). Considering these encouraging results, we extended our study to have a new insight into the cytotoxicity of one of these potent compounds.

To the best of our knowledge, the anticancer effect of compound C4 has not been reported to date. The present study was designed to investigate the *in vitro* anticancer activities of C4 on human colorectal cancer cell lines. Herein, parameters like apoptosis induction, cell cycle, oxidative stress, etc. were performed to explore the possible mechanism of cell death.

2. Materials and methods

2.1. Chemicals

Dulbecco's modified eagle medium (DMEM), RPMI-1640 medium, fetal bovine serum (FBS), phenylmethylsulfonyl fluoride (PMSF); 3–4, 5-dimethylthiazol-2-yl-2, 5-diphenyltetrazolium bromide (MTT), 2′,7′-dichlorofluorescein diacetate (DCFH-DA), propidium iodide (PI) and 5-fluorouracil (5-FU) was obtained from Sigma-Aldrich Co. LLC (ST. Louis, Mo, USA). Anti-caspase-3, anti-Bcl2, anti-Bcl-XL, anti-GAPDH, and rabbit anti-mouse horseradish peroxidase (HRP)-labeled secondary antibodies were procured from Cell Signaling Technology. Enhanced chemiluminescence (ECL) system kit, sterile filters (0.22 μm), and polyvinylidene difluoride (PVDF) membranes were procured from Millipore (MA, USA). Vybrant Apoptosis Assay Kit #2 was obtained from Molecular Probe (Eugene, Oregon, 97402-0469). Cell adhesion and cell migration kits were procured from Cell Biolabs, Inc.

2.2. Cell culture

Human colorectal adenocarcinoma HT-29 (ATCC# HTB-38) and human colorectal adenocarcinoma SW620 (ATCC# CCL-227) cells were obtained from the American Type Culture Collection (0801 University Boulevard, Manassas, VA, USA). The human normal colon epithelial cell line NCM460 was procured from Incell Corporation, LLC (San Antonio, TX, USA). The HT-29 and SW620 cells were cultured in DMEM and NCM460 cells were cultured in RPMI-1640 medium. Both the media were supplemented with 10% (v/v) FBS, 100 U/ ml penicillin and 100 μg/ ml streptomycin. All the cells were maintained at 37 °C in a humidified atmosphere containing 5% CO_2 and 95% air. The cells were screened periodically for mycoplasma contamination and maintained by routine subculturing.

2.3. Chemical synthesis

The compound C4 is one of the compounds from a group of TSC derivatives synthesized previously (Bhat et al., 2015a,b). (2Z)-N-B enzyl-2-(3-methoxybenzylidene)hydrazinecarbothioamide (4): Yield: 68%; m.p.: 127–129 °C; IR (KBr): 3148 (NH str.), 1545 (C═N str.), 1254 (NCSN str.), 1041 (C═S str.); 1H NMR (DMSO d_6); δ = 3.79 (3H, s, —OCH3), 4.8 (2H, s, —CH2), 6.9–7.4 (9H, m, Ar-H), 8.0 (1H, s, N═CH), 9.1 (1H, s, NH, D2O exchg.), 11.6 (1H, s, NHCS, D2O exchg.); 13C NMR (DMSO d_6): δ = 47.05, 55.74, 112.55, 116.04, 120.04, 120.68, 127.17, 127.63, 128.63, 130.21, 136.04, 139.91, 142.62, 160.02, 178.14; MS: m/z = 300.09 Molecules 2015, 20 18,256 [M + 1]+; Analysis: for C16H17N3OS, calcd. C 62.92, H 7.59, N 3.76, S 10.50%; found C 62.87, H 7.57, N 3.75, S 10.53%. The compound is solid and crystalline with the purity of $\geq$ 99%. Initially, C4 was dissolved in 100% DMSO as the main stock. The stock solution was diluted with < 0.1% DMEM media into concentrations from 0 to 30 μM for subsequent *in vitro* analysis.

2.4. Cell viability assay

The novel TSC derivative C4 was tested for its cytotoxicity against a panel of cancer cell lines viz., HepG2, MCF7, HT-29, SW620, and A549. Human normal colon epithelial NCM460 cells were used to examine the toxicity induced by the compound against non-cancerous human cells. Standard MTT (3–4, 5-dimethylthiazol-2-yl-2, 5-diphenyl-tetrazolium bromide) reduction assay was performed to assess the cytotoxic effect induced by C4 (Khan et al., 2019). Briefly, exponentially growing cells were seeded at 5 $\times$ 10^5 cells/200 μl in a 96-well plate in their specific growth medium. After incubation of 24 h, C4 was added in the cells at a final concentration in a range from 0 μM, 1.25 μM, 2.5 μM, 5 μM, 10 μM, 20 μM, 30 μM. After 24 h incubation, cells were replenished with a fresh growth medium and then MTT (5 mg/ ml in phosphate buffered saline (PBS)) was added at a volume of 1:10/well. The cells were again incubated for 4 h at 37 °C. The reaction was stopped by adding 100 μl DMSO after removing the medium containing MTT. The absorbance was quantified at 620 nm and was plotted as percentage values in dose–response curves. The level of cytotoxicity of the compound was measured separately

for each cell line as IC_{50} (half maximal inhibitory concentration). After determining the efficacy of C4 on cancer cells the two concentrations (5 μM and 10 μM) of compound C4 were used for further studies on the most potent cell line. Likewise, the cytotoxic effect of standard drug 5-FU (5-fluorouracil) in terms of IC_{50} values was also determined against the above-mentioned cell lines, separately.

2.5. Selectivity index

The selectivity index (SI) was determined to estimate the cytotoxic selectivity of the compound and 5-FU against tested cell lines according to (Peña-Morán et al., 2016). The SI was calculated using the IC_{50} values of C4 on the NCM460 cell line.

2.6. Analysis of cancer cell migration

Cell migration assay was carried out with a specific CytoSelect 24-Well Cell Migration Assay kit according to the manufacturer's protocol. Briefly, the lower well of the migration plate was supplemented with C4 (5 μM /10 μM) in the growth medium of respective cell lines. Cell lines at a concentration of $0.5\text{-}1x10^6$ cell/ml were added inside the insert. The migration plates were incubated for 8 h at 37 °C in a humidified CO_2 incubator. After proper processing, according to the mentioned procedure, 100 μl of each sample was transferred in a 96-well plate and quantified by taking absorbance at 560 nm (Khan et al., 2012).

2.7. Analysis of cancer cell adhesion

Cell adhesion assay was carried out with a CytoSelect 24-Well Cell Adhesion Assay kit according to the manufacturer's protocol. Briefly, $0.1–1\times10^6$ cells with 5 μM or 10 μM of C4 in one ml of serum-free medium were added to the pre-warmed ECM adhesion plate. The plates were incubated for 30–90 min in a CO_2 incubator. The wells were washed thrice with PBS and then adhered cells were stained with 200 μl of cell stain solution for 10 min at room temperature. After washing and drying the stained cells, the cells were extracted using an extraction solution and incubated for 10 min in an orbital shaker. Then 150 μl of each sample was transferred to a 96-well plate and quantified by taking absorbance at 560 nm (Khan et al., 2013).

2.8. The extent of intracellular reactive oxygen species (ROS)

The effect of C4 on the generation of ROS in HT-29 and SW620 was measured using a cell-permeable 2′,7′-dichlorofluorescein diacetate (DCFH-DA) fluorescent dye according to the published protocol (Asif et al., 2016). The HT-29 or SW620 (10×10^4cells/ well) were incubated with 5 μM and 10 μM of C4 for 24 h, separately. Thirty minutes before the end of 24 hr, DCFH-DA was added to the treated cells. After incubation, the cells were collected at 2000 rpm for 5 min at 4 °C and washed twice with PBS. DCFH-DA fluorescence was detected using a flow cytometer (MACSQuant analyzer 10, Miltenyi Biotec, Germany).

2.9. Annexin-V analysis of apoptosis

The presence of apoptotic cells was detected using the Vybrant Apoptosis Assay Kit following the published protocol (Khan et al., 2016). Briefly, the cell lines were incubated with 5 μM and 10 μM of C4 for 48 h. The cells were washed with PBS and 1×10^6 cells/ ml were incubated with annexin V-FITC and propidium iodide (PI) in dark for 15 min at room temperature. The fluorescent cells were quantified at 530–575 nm for data acquisition and analyzed on a flow cytometer.

2.10. Cell cycle analysis

The cell cycle phase distribution was investigated in HT-29 and SW620 cells after the treatment with C4. The cell lines ($5x10^5$ cells/ ml) were grown in 6-well plates for 24 h and then were treated with 5 μM and 10 μM concentrations of C4. Following desired treatment, the cells were harvested by trypsinization, washed twice with cold PBS, and fixed with 70% ethanol for 60 min at room temperature. Now, the cells were centrifuged and the pellets were suspended in PBS. The cell suspensions were incubated with 2 μl of RNase A (50 mg/ml) for 60 min at 50 °C. Next, the cells were incubated with 4 μg of PI for 30 min at room temperature. Cell cycle distribution was analyzed by a flow cytometer.

2.11. Western immunoblotting

Following desired treatment of cell lines, the cells in culture were harvested by trypsinization and washed twice in PBS. The cells were suspended in ice-cold TNN buffer (50 mM Tris-HCl pH 7.4, 100 mm NaCl, 5 mM EDTA, 0.5% Nonidet P-40, 1 μg/ ml pepstatin, 0.5 mM EGTA, 200 μM PMSF, 0.5 mM DTT and 1 μg/ ml of leupeptin) to prepare the total lysates as reported earlier (Khan et al., 2011). For Western blotting, the samples were firstly denatured in SDS-PAGE sample buffer and then electrophoresed on 10% SDS-polyacrylamide gel (Khan, 2017). The resolved proteins from the gel were electro-blotted onto the PVDF membranes and the membranes were then processed for the detection of apoptotic protein markers. Firstly, non-specific proteins present on the membranes were blocked by incubating the membranes in 5% non-fat dry milk for 1 h at room temperature. After washing thrice, the membranes were probed with primary anti-caspase-3, anti-Bcl-2, anti-Bcl-XL, and anti-GAPDH antibodies at 4 °C overnight. Immunoblots were secondary labeled with horseradish peroxidase-conjugated anti-mouse IgG secondary antibodies for 1 h and immune-reactive bands were detected by enhanced chemiluminescence (ECL) detection system (Millipore, MA, USA) with LAS 3000 imaging system (Fujifilm, Tokyo, Japan).

2.12. Statistical data analysis

All statistical analyses were conducted using Sigma-Plot 10v software. Results are expressed as mean±SD of three independent experiments. The data were statistically analyzed with Student's *t*-test or one-way ANOVA followed by Dunnett's post-hoc test. The *p* values of < 0.001, <0.01, and < 0.05 were considered statistically significant.

3. Results

3.1. Chemistry

The representative structure of C4 is shown in Scheme 1. The compound has been synthesized, characterized, and confirmed by spectral data (Bhat et al., 2015a,b). Spectral and analytical data have shown a good agreement with the composition of the synthesized C4.

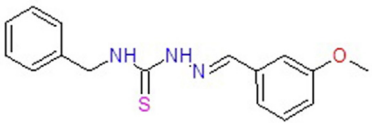

Scheme 1. The structure of thiosemicarbazone derivative C4.

3.2. Effect of C4 on tested cancer cell viability

The cytotoxic effect of C4 was tested on a panel of cancer cell lines viz., HepG2 (liver), MCF7 (breast), HT-29 (colon), and A549 (lung) as shown in Fig. 1a. This preliminary screening data revealed the potent cytotoxic activity of C4 against all the tested cancer cell lines. Notably, C4 induced relatively weak cytotoxicity in the non-cancerous colon epithelial NCM460 cell line. Increasing concentration of C4 from 0 to 30 μM depicted a dose-dependent decrease in cancer cell viability. However, as shown in Table 1, the order of sensitivity varied where HT-29 (IC_{50} value 6.7 μM) was most potent to the cytotoxic effect of C4 followed by MCF7 (IC_{50} value 14.5 μM), HepG2 (IC_{50} value 16.8 μM) and A549 (IC_{50} value 23.7 μM). 5-FU was found to have significant indiscriminate cytotoxicity against cancer cells as well as a non-cancerous cell type (Table 1).

Considering the lowest IC_{50} value obtained, we continued our study on colon cancer cells. The growth inhibition effects of C4 were investigated on cell lines *viz.* colorectal cancer cell line HT-29 and metastasis specific colorectal cancer cell line SW620. Fig. 1b shows that the C4 treatment significantly inhibited cell viability in a dose-dependent manner. A relatively low cytotoxic dose of the compound displayed high cytotoxic activity. IC_{50} value showed that C4 had more potent inhibitory effects on HT-29 cells (IC_{50} = 6.7 μM) than SW620 cells (IC_{50} = 8.3 μM). In response to 6.7 μM, the growth rate of HT-29 was 49.68% whereas SW620 at 8.3 μM showed a growth rate of 47.53%.

3.3. Effect of C4 on tested cancer cell selectivity

The SI of C4 and standard against various cancer cells are shown in Table 1. The selectivity index shows that C4 was more selective for cancer cells than non-cancerous cell, in contrast to standard 5-FU, which have lower efficacy. Compound C4 had the highest selectivity index against the HT-29 and SW620 cell lines (14.92 and 12.04 respectively), as demonstrated in Table 1.

3.4. Effect of C4 on colon cancer cell migration

As shown in Fig. 2, C4 significantly inhibited the migration of HT-29 cells in a dose-dependent manner. The number of migrating cells was reduced to about 40.65% at 5 μM and 56.95% at 10 μM, compared to the untreated control group. C4 exhibited similar inhibitory effects on the migration of SW620 cells (Fig. 2). As compared with the untreated control group, cell migration was decreased to 34.79% and 46.48%, in response to 5 μM and 10 μM of C4 treatment.

Table 1
IC_{50} values and selectivity index of compound C4 and 5-fluorouracil treated cancer cells.

Cell lines	IC_{50} (μM)		SI	
	C4	5-FU	C4	5-FU
A549	23.7 ± 5.3	8.3 ± 1.2	4.22	1.27
MCF7	14.5 ± 1.6	3.2 ± 0.2	6.89	3.31
HepG2	16.8 ± 3.2	3.4 ± 0.5	5.95	3.11
HT-29	6.7 ± 0.7	4.1 ± 0.3	14.92	2.58
SW620	8.3 ± 0.3	5.7 ± 0.5	12.04	1.85
NCM460	>100	10.60 ± 6.2		

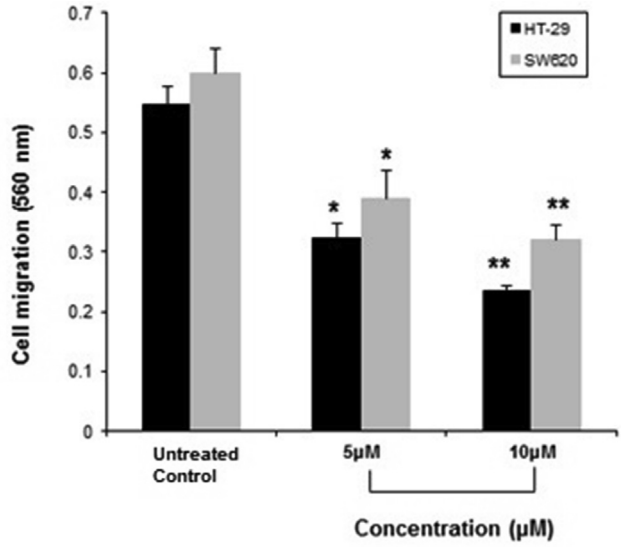

Fig. 2. The inhibitory effect of C4 on the migration of HT-29 and SW620 colon cancer cells following treatment with 5 μM and 10 μM concentrations. Results are expressed as mean±SD of three independent experiments. $^{*}p < 0.05$ and $^{**}p < 0.01$ for colon cancer cells versus untreated control were considered significant.

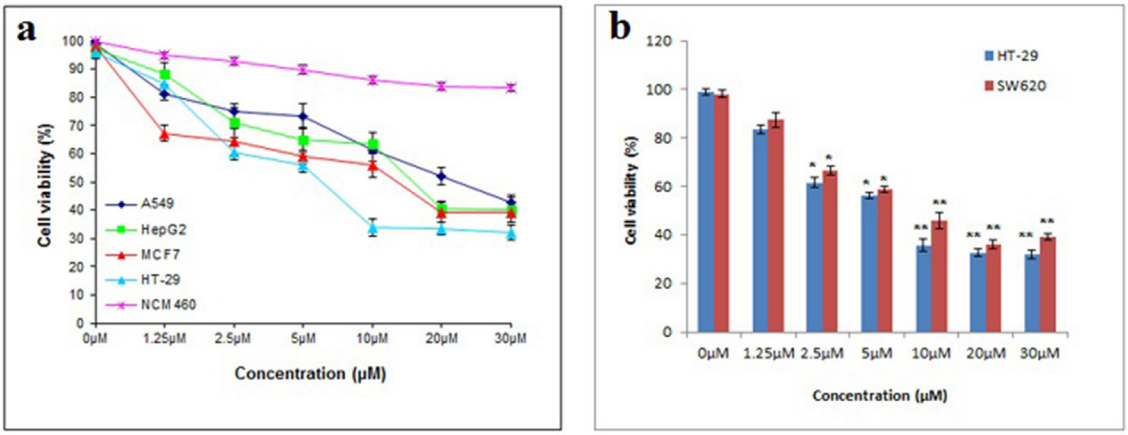

Fig. 1. (a) The inhibitory effect of C4 on the viability of various cancer cells viz., HepG2, MCF7, HT-29, A549, and NCM460 normal cells. Cells were treated with 0–30 μM range of C4 concentration and then assessed using MTT assay. (b) Cell viability was compared between HT-29 and SW620 colon cancer cells following treatment with a 0–30 μM range of C4 concentration. Results are expressed as mean±SD of three independent experiments. $^{*}p < 0.05$ and $^{**}p < 0.01$ for colon cancer cells versus untreated control were considered significant.

3.5. Effect of C4 on colon cancer cell adhesion

The effect of C4 was examined on cancer cell adhesion. The C4 treatment inhibited the adhesion of HT-29 and SW620 cells in a dose-dependent manner (Fig. 3). In comparison to the untreated control, the inhibition rate of HT-29 cell adhesion in response to 5 μM and 10 μM concentrations of C4 was 23.48% and 42.1%, respectively. The inhibition rate for SW620 was 28.84% and 38.07% at a treatment dose of 5 μM and 10 μM, respectively.

3.6. Effect of C4 on ROS generation in colon cancer cells

To identify whether the cytotoxic stimuli induced by C4 in colon cancer cells were mediated through oxidative stress, DCFH-DA was used to measure the generation of intracellular ROS in HT-29 and SW620 cells. As shown in Fig. 4A, HT-29 cells exhibited a steady increase in DCF fluorescence intensity when treated with 5 μM and 10 μM concentrations of C4. Compared to untreated control, the intracellular ROS increased significantly to 78.22% and 83.70% after exposure to 5 μM and 10 μM, respectively. In SW620 cells also, a significant increase in the DCF fluorescence signal was observed in comparison with the untreated control (Fig. 4B). There was a 90.55% (5 μM) and 86.94% (10 μM) increase in intracellular ROS levels in SW620 cells.

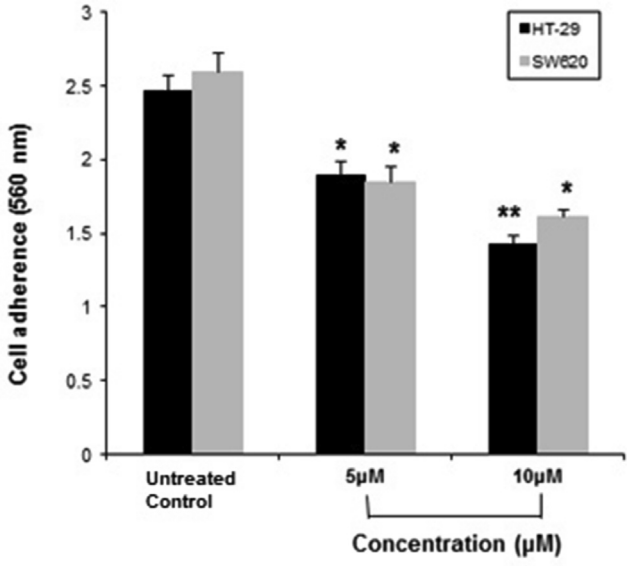

Fig. 3. The inhibitory effect of C4 on adhesion of HT-29 and SW620 colon cancer cells following treatment with 5 μM and 10 μM concentrations. Results are expressed as mean±SD of three independent experiments. $^{*}p < 0.05$ and $^{**}p < 0.01$ for colon cancer cells versus untreated control were considered significant.

3.7. Effect of C4 on apoptosis induction in colon cancer cells

Since a significant reduction in cell viability was observed after C4 treatment, we evaluated the effect of C4 on the induction of apoptosis in HT-29 and SW620 cells by Annexin V-PI staining. Figs. 5 and 6 show the flow cytometric diagrams of the apoptotic morphological changes of cells after treatment with C4. A distinct decrease in viability and increase in apoptosis was observed in treated cancer cells (Annexin $V^{+}PI^{-}$) in comparison to the untreated cells where almost 95% of the cells were viable and non-apoptotic (Annexin $V^{-}PI^{-}$). In HT-29 cells, with the increase in the concentration of C4, there was a steady increase in the annexin positive cells (Fig. 5). After treatment with 10 μM, the population of early apoptotic cells (Annexin $V^{+}PI^{-}$) increased from 28.88% (5 μM) to 39.59%. The percentage of late apoptotic cells (Annexin $V^{+}PI^{+}$) also increased from 21.29% (5 μM) to 31.92% (10 μM).

Obtained results of SW620 cells, also indicated that the cells undergo apoptosis when they were treated with C4 (Fig. 6). The percentage of early apoptotic cell population increased from 19.62% (5 μM) to 46.59% (10 μM). With an increase in concentration from 5 μM to 10 μM, there was a distinct increase in the Annexin $V^{+}PI^{+}$ late apoptotic cells (11.06–21.07%, respectively). The analysis also specified that there was negligible necrosis.

3.8. Effect of C4 on colon cancer cell cycle

Since Annexin V-PI staining assay suggested an effect of C4 on the induction of apoptosis, we performed FACS analysis to determine the effect of C4 on the cell cycle progression. Interestingly, after treatment of HT-29 and SW620 cells with C4, a concentration-dependent change was observed in the cell cycle phase distribution (Fig. 7). As compared to untreated control, cell

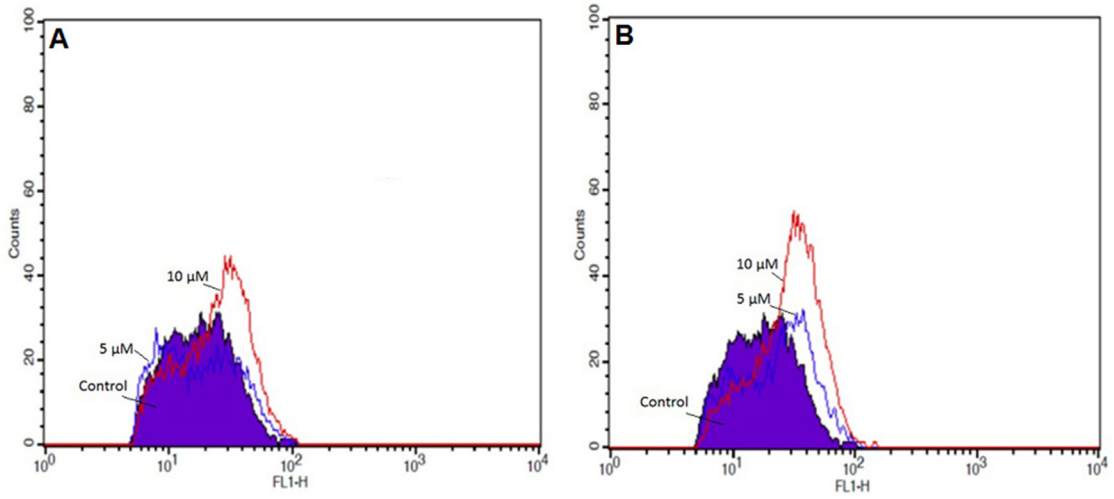

Fig. 4. The effect of C4 on ROS levels in HT-29 and SW620 colon cancer cells following the treatment with 5 μM and 10 μM concentrations of C4. The ROS levels were analyzed by flow cytometry after staining with DCFH-DA.

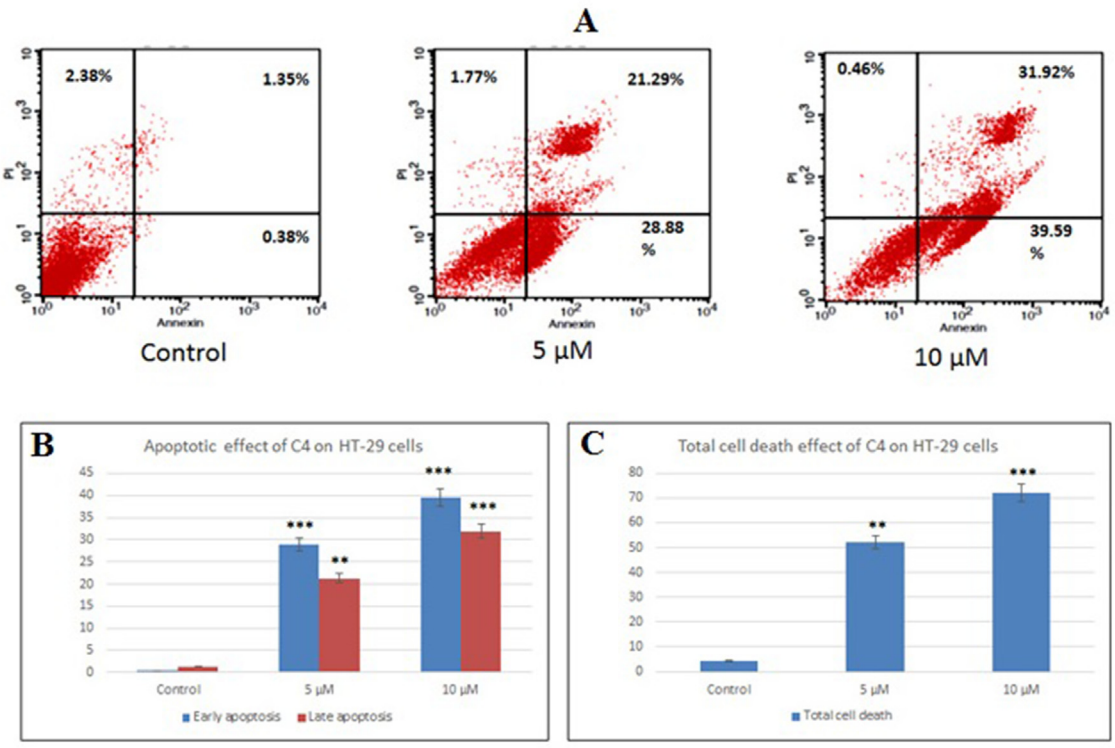

Fig. 5. The apoptotic effect of C4 on HT-29 colon cancer cells was quantified by Annexin V-PI staining assay. (A) Flow cytometry charts of HT-29 cells representing untreated control, treated with 5 µM C4 and treated with 10 µM C4, respectively. Graphs show (B) percent apoptosis and (C) percent total cell death of HT-29 cells following treatment with 5 µM and 10 µM C4 concentrations. Results are expressed as mean±SD of three independent experiments. $^{**}p < 0.01$ and $^{***}p < 0.001$ for HT-29 cells versus untreated control were considered significant.

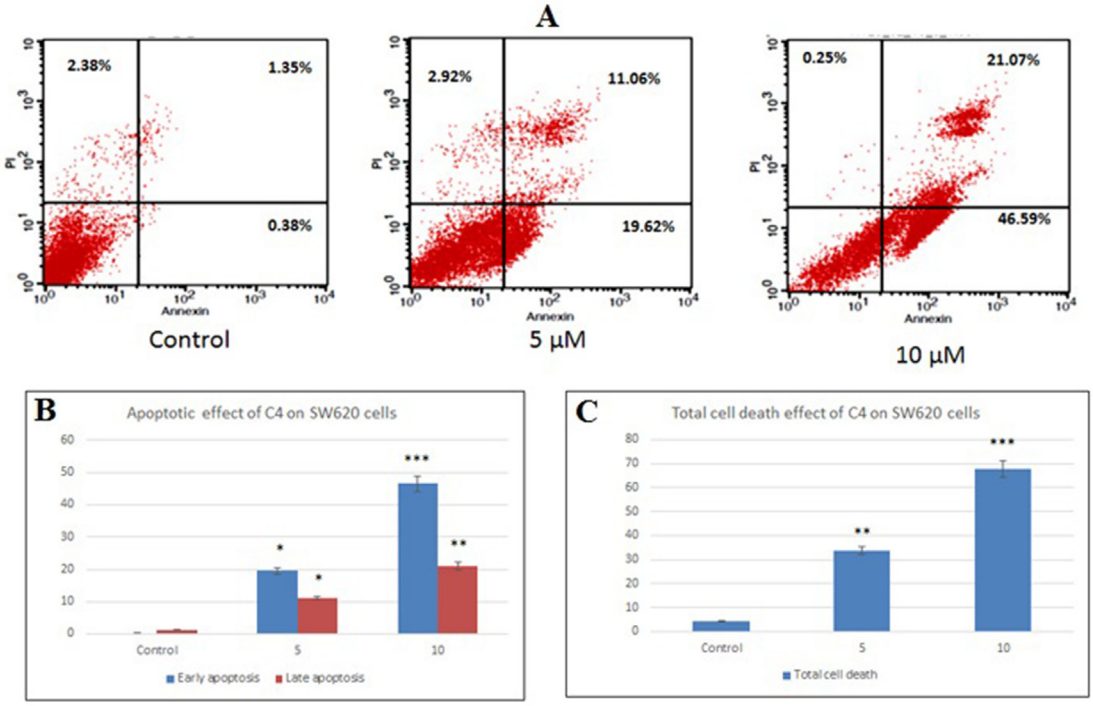

Fig. 6. The apoptotic effect of C4 on SW620 colon cancer cells was quantified by Annexin V-PI staining assay. (A) Flow cytometry charts of SW620 cells representing untreated control, treated with 5 µM C4 and treated with 10 µM C4, respectively. Graphs show (B) percent apoptosis and (C) percent total cell death of SW620 cells following treatment with 5 µM and 10 µM C4 concentrations. Results are expressed as mean±SD of three independent experiments. $^{*}p < 0.05$, $^{**}p < 0.01$ and $^{***}p < 0.001$ for SW620 cells versus untreated control were considered significant.

cycle analysis showed a considerable increment of cell population in the subG1 phase, indicating the accumulation of apoptotic cells. A percentage of apoptotic cells increased in a concentration-dependent manner from 11.74% (control) to 61.61% (5 μM) and 68.27% (10 μM) in HT-29 cells and 52.91% (5 μM) and 56.25% (10 μM) in SW620 cells. A significant decrease in the cell population in the G2/M phase was also seen in C4-treated cells. As compared to the untreated control cells (35.28%) in the G2/M phase, cell population decreased to 10.49% (5 μM) and 4.77% (10 μM) in HT-29 cells and 12.66% (5 μM) and 10.31% (10 μM) in SW620 cells. Our results hence imply induction of apoptotic cell death and an arrest of cell cycle progression at the G2/M phase.

3.9. Effect of C4 on apoptotic factors in colon cancer cells

To determine the possible mechanism by which C4 triggers apoptosis in HT-29 and SW620 cells, we assessed the expression of pro-and anti-apoptosis regulating protein markers. Fig. 8 shows the results of Western blot analysis of anti-apoptotic Bcl-XL and Bcl-2 proteins; and pro-apoptotic caspase-3 protein. Compared to the untreated controls, the C4 treatment down-regulated the protein levels of Bcl-XL and Bcl-2 after treatment with 5 μM and 10 μM concentrations in both the cell lines. The treatment with C4 showed a significantly strong decrease in the Bcl-2 levels from 60.81% (5 μM) to 1.13% (10 μM) in HT-29 cells. A significant decline in Bcl-2 expression levels in SW620 cells was also observed from 85.88% (5 μM) to 61.96% (10 μM). In comparison to the untreated control, a moderate increase of 7.12% was observed in Bcl-XL levels at 5 μM in HT-29 cells. However, the levels significantly dropped to 36.89% at 10 μM as compared to untreated control. In SW620 cells, expression of Bcl-XL decreased to 36.84% (5 μM) and 53.15% (10 μM) upon comparison with the untreated control. Furthermore, in both HT-29 and SW620 cell lines, C4 treatment up-regulated the expression level of caspase-3 protein as compared to the untreated control. There was a significant dose-dependent increase in the caspase-3 levels from 23.23% (5 μM) to 56.9% (10 μM) and 19.62% (5 μM) to 51.85% (10 μM) in HT-29 and SW620 cells, respectively.

4. Discussion

Thiosemicarbazones and their derivatives are widely acknowledged as a well-known class of compounds bearing potent anticancer ability (Kalinowski et al., 2009; Moorthy et al., 2013). In the current study, we have tried to investigate the anticancer potential of a novel 2-cyclohexyl-N-[(Z)-(3-methoxyphenyl)-methylidene] hydrazinecarbothioamide (C4) compound and its possible mechanism of action against colon cancer cells. Primarily, C4

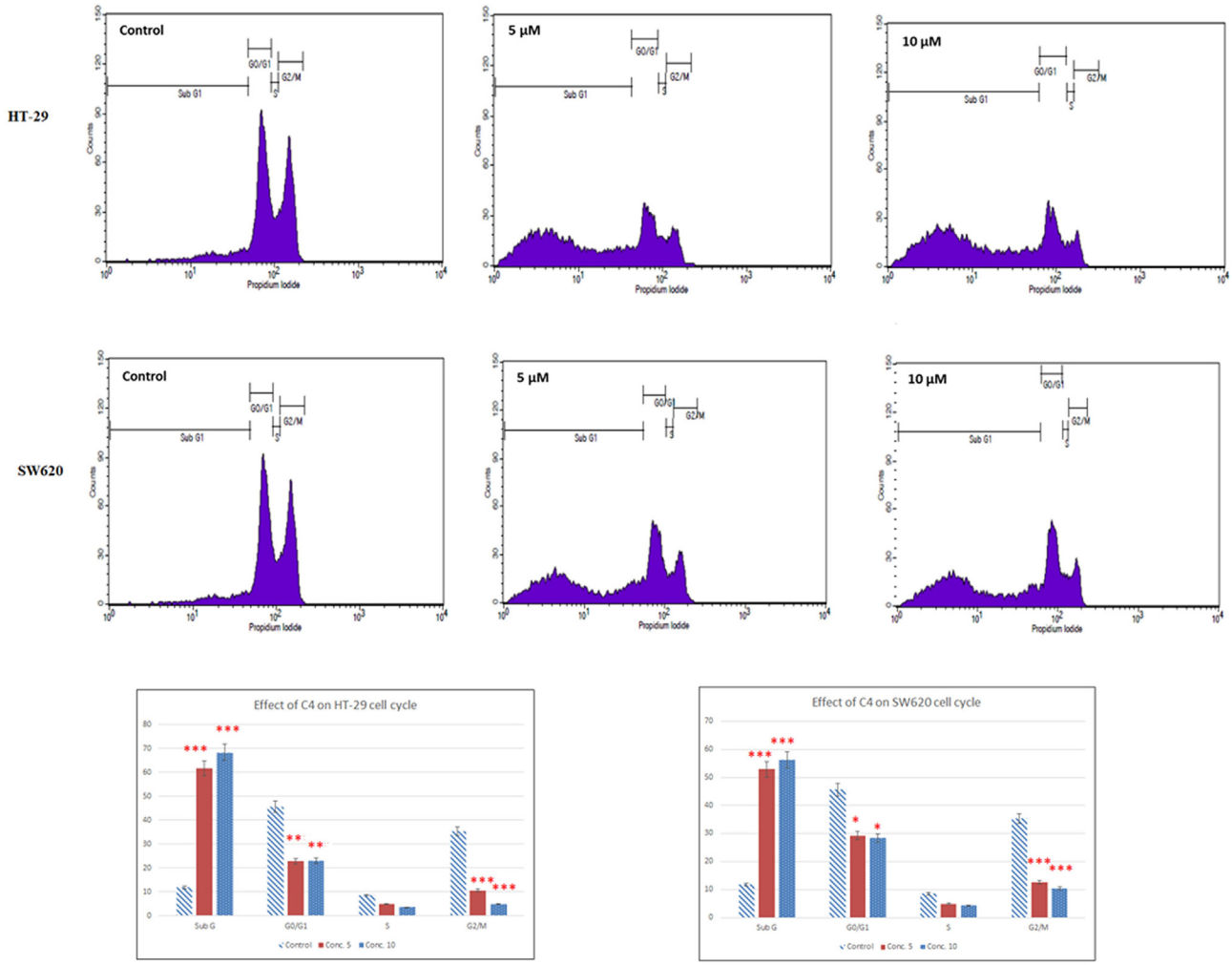

Fig. 7. Cell cycle analysis of HT-29 and SW620 colon cancer cells following treatment with 5 μM and 10 μM concentrations. Histograms show the percentage of cells in the G0/G1, G1, S, and G2/M phases of the cell cycle obtained after FACS analysis. Results are expressed as mean±SD of three independent experiments. $^{*}p < 0.05$, $^{**}p < 0.01$and $^{***}p < 0.001$ for colon cancer cells versus untreated control were considered significant.

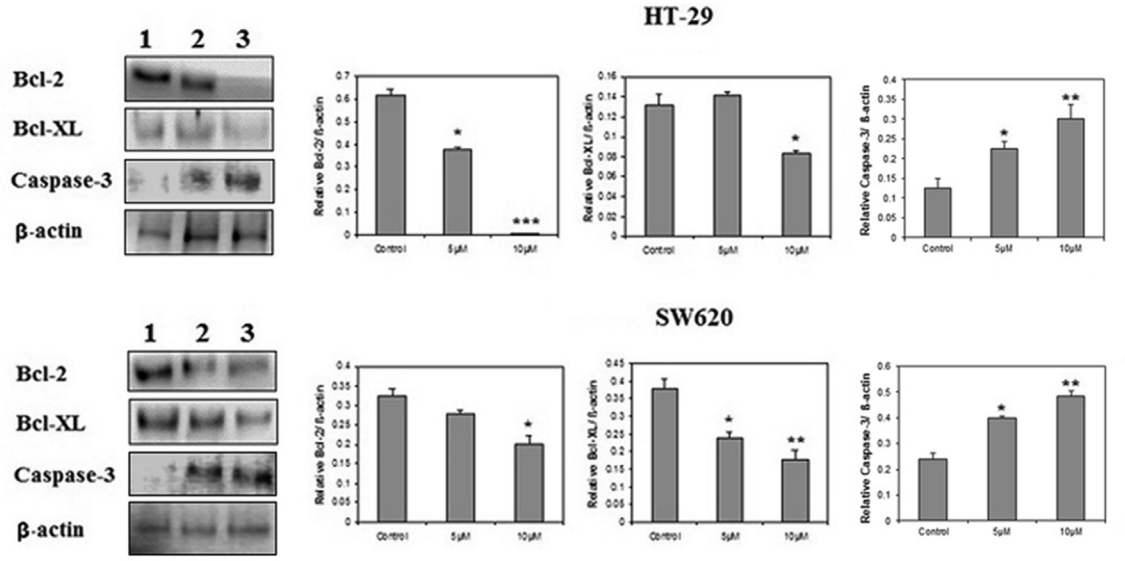

Fig. 8. Effect of C4 on the modulation of apoptotic factors on HT-29 and SW620 colon cancer cells following the treatment with 5 μM and 10 μM concentrations. Western blots show expression of Bcl-2, Bcl-XL, and caspase-3 in Lanes, (1) untreated control; (2) cells treated with 5 μM of C4 and (3) cells treated with 10 μM of C4. Densitograms show percent expression of Bcl-2, Bcl-XL, and caspase-3 in HT-29 and SW620 cells. Results are expressed as mean ± SD of three independent experiments. $^{*}p < 0.05$, $^{**}p < 0.01$ and $^{***}p < 0.001$ for colon cancer cells versus untreated control were considered significant.

demonstrated potent cytotoxic action on the panel of cancer cell lines *viz*., HepG2, MCF7, HT-29, SW620, and A549 (IC_{50} values from 14 μM to 25 μM) whereas the minimum effect was noted on NCM460 normal cells (Fig. 1a). Among the tested cancer cell lines, HT-29 cells were found to be the most susceptible ones with an IC_{50} value of 6.7 μM. To represent any novel compound as an anticancer agent, the compound must be able to act on different stages of cancer. Hence, we tried to determine the anticancer potential of C4 against two colorectal cancer cell lines *viz*., HT-29 (representing primary localized stage) and SW620 (representing advanced metastatic stage). As evident from the MTT result, C4 inhibited the viability of SW620 cells also (IC_{50} value 8.3 μM).

The possible molecular mechanism used by TSCs in a cell by far is unsatisfactorily clear. Various studies have demonstrated that TSCs can act on different pathways (Gutierrez et al., 2016; Kovacevic et al., 2011). Since there was a significant decrease in cell viability after treatment with C4, we employed different parameters to investigate the C4 effect on the two colorectal cancer cells HT-29 and SW620. The malignant tumor cells are survived by exhibiting two essential activities i.e. adhesion and migration. Cell migration is one of the main reasons for mortality in cancer patients (Cheng et al., 2007). Herein, C4 significantly inhibited the migration and adhesion of both HT-29 and SW620 cells in a dose-dependent manner (Figs. 2 and 3, respectively). Among various methods in controlling the proliferation of cancer cells, apoptosis is one of the main approaches employed (Ziegler and Kung, 2008). Most of the metal-based anticancer drugs have shown their cytotoxic effect through apoptosis. As evident from our Annexin V data (Figs. 5 and 6), we observed that C4 inhibited the growth and induced apoptosis in both HT-29 and SW620 cells in a dose-dependent manner. The morphological study proved that the cytotoxic effect of C4 is primarily due to apoptosis and not necrosis.

ROS are considered an important representative of a cell's metabolic status. They act as apoptosis inducers in most of the physiological and pathological conditions (Andrienko et al., 2016). Usually, the chemical compounds increase the intracellular ROS levels that result in apoptosis induction and cell death (Redza-Dutordoira and Averill-Bates, 2016). To date, most of the TSC compounds are reported to display the generation of intracellular ROS as a main pharmacological effect in cancer proliferation (Huang et al., 2010; Kalinowski et al., 2007). Hence, determining the ROS levels is an important parameter for investigating the mechanism of compound-induced apoptosis. In the present study, there was a steady increase in the production of ROS in HT-29 and SW620 cells after exposure to C4. In comparison to untreated cells, the levels of ROS increased with an increase in the concentration of C4. These results suggest that the anticancer ability of C4 might require the generation of ROS to induce apoptosis in cancer cells.

Cell cycle arrest is one of the mechanisms that are looked at during the development of an anticancer drug. Several reports have shown the potential anticancer effect of metal-based derivatives on the cell cycle (Abbaszadeh et al., 2020; Irace et al., 2017; Malarz et al., 2018; Shahrokhshahi et al., 2021; Song et al., 2020). Since C4 was efficient in inhibition of cell viability through excess production of ROS we evaluated the effect of C4 on the cell cycle arrest. The results demonstrated that at 5 μM and 10 μM concentrations, C4 interfered in the cell cycle distribution in a dose-dependent manner. Compared with the untreated control, the cell population decreased in G0/G1 and S phase and were arrested in the G2/M phase in both HT-29 and SW620 cells (Fig. 6). These findings indicate that the anticancer effect of C4 on colon cancer cells could be attributed to the block in cell cycle progression.

Since C4 treatment resulted in the potential induction of apoptosis, we subsequently investigated the effect of C4 on various apoptosis regulating proteins. The triggering of the apoptotic process is regulated by four major functional groups of molecules like caspases, the Bcl-2 family of proteins, adaptor proteins, and the tumor necrosis factor receptor family. Since it is a known fact that these actions are concomitant to the mitochondrial signaling pathway and consequently depict changes in the expression and post-transcriptional modifications of anti-apoptotic (Bcl-2 and Bcl-xL) and pro-apoptotic (Bad and Bax) proteins (Chipuk et al., 2010). In our study, C4 inhibited Bcl-XL and Bcl-2 expression in HT-29 and SW620 cells. (Fig. 8). From these results, it can be envisaged that modulation of Bcl-2 family proteins will trigger the release of cytochrome *c* from mitochondria thereby activating the cascade of cas-

pases. Since, caspases are an integral part of apoptosis, their activation act as the trigger for cell death (Logue and Martin, 2008). Herein, both tested concentrations of C4 induced apoptotic death by activation of caspase-3 in both HT-29 and SW620 cells (Fig. 8). Overall, these results indicate that C4 induced cell death through an apoptotic pathway in both HT-29 and SW620 colon cancer cells.

5. Conclusions

The results of the present study highlight that the novel C4 compound belonging to the group of synthesized TSC derivatives bearing cyclohexyl moiety possesses potential anti-cancer properties and can be considered a promising anticancer agent. The compound showed cytotoxicity to a panel of cancer cells and caused effective inhibition of colon cancer cell adhesion and migration. Exposure of the HT-29 and SW620 cells to C4 induced significant generation of ROS and caused cell cycle arrest at the G2/M phase. C4 also regulated the caspase-3, Bcl-2, and Bcl-XL genes in HT-29 and SW620 cells and induced apoptotic cell death. The findings of the current study can be utilized as prospective therapeutic in the treatment of colon cancer.

Funding

This research was funded by the Researchers Supporting Project Number (RSP-2021/339) at King Saud University.

Informed Consent Statement

Not applicable.

Data Availability Statement

The data presented in this study are available in this article.

Declaration of Competing Interest

The authors declare that they have no known competing financial interests or personal relationships that could have appeared to influence the work reported in this paper.

References

Abbaszadeh, N., Jaahbin, N., Pouraei, A., Mehraban, F., Hedayati, M., Majlesi, A., Akbari, F., Sadat Shandiz, S.A., Salehzadeh, A., 2020. Preparation of novel nickel oxide@ glutamic/thiosemicarbazide nanoparticles: Implications for cytotoxic and anti-cancer studies in MCF-7 breast cancer cells. J. Clust. Sci. 33 (2), 457–465.

Andrienko, T., Pasdois, P., Rossbach, A., Halestrap, A.P., 2016. Real-time fluorescence measurements of ROS and [Ca2+] in ischemic/reperfused rat hearts: Detectable increases occur only after mitochondrial pore opening and are attenuated by ischemic preconditioning. PLoS One 11(12), e167300.

Asif, M., Yehya, A.H.S., Al-Mansoub, M.A., Revadigar, V., Ezzat, M.O., Ahamed, M.B.K., Oon, C.E., Murugaiyah, V., Majid, A.S.A., Majid, A.M.S.A., 2016. Anticancer attributes of *Illicium verum* essential oils against colon cancer. S. Afr. J. Bot. 103, 156–161.

Bejarbaneh, M., Moradi-Shoeili, Z., Jalali, A., Salehzadeh, A., 2020. Synthesis of cobalt hydroxide nano-flakes functionalized with glutamic acid and conjugated with thiosemicarbazide for anticancer activities against human breast cancer cells. Biol. Trace Elem. Res. 198 (1), 98–108.

Bhat, M.A., Al-Dhfyan, A., Khan, A.A., Al-Harbi, N., Manogaran, P.S., Alanazi, A.M., Fun, H.-K., Al-Omar, M.A., 2015a. Targeting HER-2 over expressed breast cancer cells with 2-cyclohexyl-N-[(Z)-(substituted phenyl/furan-2-yl/thiophene-2-yl) methylidene]hydrazinecarbothioamide. Bioorg. Med. Chem. Lett. 25 (1), 83–87.

Bhat, M.A., Al-Dhfyan, A., Naglah, A.M., Khan, A.A., Al-Omar, M.A., 2015b. Lead optimization of 2-cyclohexyl-N-[(Z)-(3-methoxyphenyl/3hydroxyphenyl) methylidene]hydrazinecarbothioamides for targeting the HER-2 overexpressed breast cancer cell line SKBr-3. Molecules. 20, 18246–18263.

Boursi, B., Arber, N., 2007. Current and future clinical strategies in colon cancer prevention and the emerging role of chemoprevention. Curr. Pharm. Des. 13, 2274–2282.

Cheng, G.Z., Chan, J., Wang, Q., Zhang, W., Sun, C.D., Wang, L.H., 2007. Twist transcriptionally up-regulates AKT2 in breast cancer cells leading to increased migration, invasion, and resistance to paclitaxel. Cancer Res. 67 (5), 1979–1987.

Chipuk, J.E., Moldoveanu, T., Llambi, F., Parsons, M.J., Green, D.R., 2010. The BCL-2 family reunion. Mol. Cell. 37 (3), 299–310.

Dong, G., Wu, Y., Sun, Y., Liu, N., Wu, S., Zhang, W., Sheng, C., 2018. Identification of potent catalytic inhibitors of human DNA topoisomerase II by structure-based virtual screening. Med. Chem. Comm. 9, 1142–1146.

Ferlay, J., Colombet, M., Soerjomataram, I., Mathers, C., Parkin, D.M., Piñeros, M., Znaor, A., Bray, F., 2019. Estimating the global cancer incidence and mortality in 2018: GLOBOCAN sources and methods. Int. J. Cancer 144 (8), 1941–1953.

Finch, R.A., Liu, M.-C., Grill, S.P., Rose, W.C., Loomis, R., Vasquez, K.M., Cheng, Y.-C., Sartorelli, A.C., 2000. Triapine (3-aminopyridine-2-carboxaldehyde-thiosemicarbazone): A potent inhibitor of ribonucleotide reductase activity with broad spectrum antitumor activity. Biochem. Pharmacol. 59 (8), 983–991.

Giacchetti, S., Itzhaki, M., Gruia, G., Adam, R., Zidani, R., Kunstlinger, F., Brienza, S., Alafaci, E., Bertheault-Cvitkovic, F., Jasmin, C., Reynes, M., Bismuth, H., Misset, J. L., Lévi, F., 1999. Long-term survival of patients with unresectable colorectal cancer liver metastases following infusional chemotherapy with 5-fluorouracil, leucovorin, oxaliplatin and surgery. Ann. Oncol. 10 (6), 663–669.

Giuliani, F., De Vita, F., Colucci, G., Pisconti, S., 2010. Maintenance therapy in colon cancer. Cancer Treat. Rev. 36 (3), S42–S45.

Gutierrez, E.M., Seebacher, N.A., Arzuman, L., Kovacevic, Z., Lane, D.J.R., Richardson, V., Merlot, A.M., Lok, H., Kalinowski, D.S., Sahni, S., Jansson, P.J., Richardson, D.R., 2016. Lysosomal membrane stability plays a major role in the cytotoxic activity of the anti-proliferative agent, di-2-pyridylketone 4,4-dimethyl-3-thiosemicarbazone (Dp44mT). Biochim. Biophys. Acta. 1863, 1665–1681.

Habibi, A., Sadat Shandiz, S.A., salehzadeh, A., Moradi-Shoeili, Z., 2020. Novel pyridinecarboxaldehyde thiosemicarbazone conjugated magnetite nanoparticulates (MNPs) promote apoptosis in human lung cancer A549 cells. J. Biol. Inorg. Chem. 25 (1), 13–22.

Habibzadeh, S.Z., Salehzadeh, A., Moradi-Shoeili, Z., et al., 2020. A novel bioactive nanoparticle synthesized by conjugation of 3-chloropropyl trimethoxy silane functionalized Fe_3O_4 and 1-((3-(4-chlorophenyl)-1-phenyl-1H-pyrazol-4-yl) methylene)-2-(4-phenylthiazol-2-yl) hydrazine: assessment on anti-cancer against gastric AGS cancer cells. Mol. Biol. Rep. 47, 1637–1647.

Huang, H., Chen, Q., Ku, X., Meng, L., Lin, L., Wang, X., Zhu, C., Wang, Y., Chen, Z., Li, M., Jiang, H., Chen, K., Ding, J., Liu, H., 2010. A series of alpha-heterocyclic carboxaldehyde thiosemicarbazones inhibit topoisomerase IIalpha catalytic activity. J. Med. Chem. 53 (8), 3048–3064.

Irace, C., Misso, G., Capuozzo, A., Piccolo, M., Riccardi, C., Luchini, A., Caraglia, M., Paduano, L., Montesarchio, D., Santamaria, R., 2017. Antiproliferative effects of ruthenium-based nucleolipidic nanoaggregates in human models of breast cancer in vitro: insights into their mode of action. Sci. Rep. 7, 45236.

Jarestan, M., Khalatbari, K., pouraei, A., Sadat Shandiz, S.A., Beigi, S., Hedayati, M., Majlesi, A., Akbari, F., Salehzadeh, A., 2020. Preparation, characterization, and anticancer efficacy of novel cobalt oxide nanoparticles conjugated with thiosemicarbazide. 3. Biotech 10 (5). https://doi.org/10.1007/s13205-020-02230-4.

Jemal, A., Siegel, R., Ward, E., Hao, Y., Xu, J., Thun, M.J., 2009. Cancer statistics, 2009. CA Cancer J. Clin. 59, 225–249.

Jung, G.R., Kim, K.J., Choi, C.H., Lee, T.B., Han, S.I., Han, H.K., Han, H.K., Lim, S.C., 2007. Effect of betulinic acid on anticancer drug-resistant colon cancer cells. Basic Clin. Pharmacol. Toxicol. 101 (4), 277–285.

Kalinowski, D., Yu, Y., Sharpe, P., Islam, M., Liao, Y.-T., Lovejoy, D.B., Kumar, N., Bernhardt, P.V., Richardson, D.R., 2007. Design, synthesis, and characterization of novel iron chelators: structure-activity relationships of the 2-benzoylpyridine thiosemicarbazone series and their 3-nitrobenzoyl analogues as potent antitumor agents. J. Med. Chem. 50 (15), 3716–3729.

Kalinowski, D.S., Quach, P., Richardson, D.R., 2009. Thiosemicarbazones: the new wave in cancer treatment. Future Med. Chem. 1 (6), 1143–1151.

Karp, J.E., Giles, F.J., Gojo, I., Morris, L., Greer, J., Johnson, B., Thein, M., Sznol, M., Low, J., 2008. A phase I study of the novel ribonucleotide reductase inhibitor 3-aminopyridine-2-carboxaldehyde thiosemicarbazone (3-AP, Triapine) in combination with the nucleoside analog fludarabine for patients with refractory acute leukemias and aggressive myeloproliferative disorders. Leuk Res. 32 (1), 71–77.

Khan, A.A., Alam, M., Tufail, S., Mustafa, J., Owais, M., 2011. Synthesis and characterization of novel PUFA esters exhibiting potential anticancer activities: An in vitro study. Eur. J. Med. Chem. 46, 4878–4886.

Khan, A.A., Husain, A., Jabeen, M., Mustafa, J., Owais, M., 2012. Synthesis and characterization of novel n-9 fatty acid conjugates possessing antineoplastic properties. Lipids 47, 973–986.

Khan, A.A., Alanazi, A.M., Jabeen, M., Chauhan, A., Abdelhameed, A.S., 2013. Design, synthesis and in vitro anticancer evaluation of a stearic acid-based ester conjugate. Anticancer Res. 33, 2517–2524.

Khan, A.A., Alanazi, A.M., Jabeen, M., Hassan, I., Bhat, M.A., 2016. Targeted nano-delivery of novel omega-3 conjugate against hepatocellular carcinoma: Regulating COX-2/bcl-2 expression in an animal model. Biomed. Pharmacother. 81, 394–401.

Khan, A.A., 2017. Pro-apoptotic activity of nano-escheriosome based oleic acid conjugate against 7, 12-dimethylbenz (a) anthracene (DMBA) induced cutaneous carcinogenesis. Biomed. Pharmacother. 90, 295–302.
Khan, A.A., Alanazi, A.M., Jabeen, M., Chauhan, A., Ansari, M.A., 2019. Therapeutic potential of functionalized siRNA nanoparticles on regression of liver cancer in experimental mice. Sci. Rep. 9 (1), 15825–15840.
Kovacevic, Z., Chikhani, S., Lovejoy, D.B., Richardson, D.R., 2011. Novel thiosemicarbazone iron chelators induce up-regulation and phosphorylation of the metastasis suppressor N-myc down-stream regulated gene 1: a new strategy for the treatment of pancreatic cancer. Mol. Pharmacol. 80 (4), 598–609.
Lee, B.M., Park, K.K., 2003. Beneficial and adverse effects of chemopreventive agents. Mutat. Res. 523–524, 265–278.
Linciano, P., Moraes, C.B., Alcantara, L.M., Franco, C.H., Pascoalino, B., Freitas-Junior, L.H., Paola Costi, M., 2018. Aryl thiosemicarbazones for the treatment of trypanosomatidic infections. Eur. J. Med. Chem. 146, 423–434.
Logue, S.E., Martin, S.J., 2008. Caspase activation cascades in apoptosis. Biochem. Soc. Trans. 36, 1–9.
Lukmantara, A.Y., Kalinowski, D.S., Kumar, N., Richardson, D.R., 2013. Synthesis and biological evaluation of substituted 2-benzoylpyridine thiosemicarbazones: novel structure–activity relationships underpinning their anti-proliferative and chelation efficacy. Bioorg. Med. Chem. Lett. 23 (4), 967–974.
Ma, B., Goh, B.C., Tan, E.H., Lam, K.C., Soo, R., Leong, S.S., Wang, L.Z., Mo, F., Chan, A.T. C., Zee, B., Mok, T., 2008. A multicenter phase II trial of 3-aminopyridine-2-carboxaldehyde thiosemicarbazone (3-AP, Triapine®) and gemcitabine in advanced non-small-cell lung cancer with pharmacokinetic evaluation using peripheral blood mononuclear cells. Invest. New Drugs 26 (2), 169–173.
Malarz, K., Mrozek-Wilczkiewicz, A., Serda, M., Rejmund, M., Polanski, J., Musiol, R., 2018. The role of oxidative stress in activity of anticancer thiosemicarbazones. Oncotarget. 9 (25), 17689–17710.
Montazeri, A., Salehzadeh, A., Zamani, H., 2020. Effect of silver nanoparticles conjugated to thiosemicarbazide on biofilm formation and expression of intercellular adhesion molecule genes, icaAD, in Staphylococcus aureus. Folia Microbiol. 65, 153–160.
Montazeri, A., Zamani, H., Salehzadeh, A., 2019. Synergistic antimicrobial potential of ciprofloxacin with silver nanoparticles conjugated to thiosemicarbazide against ciprofloxacin resistant Pseudomonas aeruginosa by attenuation of MexA-B efflux pump genes. Biologia 74, 1191–1196.
Moorthy, N.S.H.N., Cerqueira, N.M.F.S.A., Ramos, M.J., Fernandes, P.A., 2013. Aryl- and heteroaryl-thiosemicarbazone derivatives and their metal complexes: a pharmacological template. Recent Pat. Anti-Cancer Drug Discov. 8 (2), 168–182.
Murren, J., Modiano, M., Clairmont, C., Lambert, P., Savaraj, N., Doyle, T., Sznol, M., 2003. Phase I and pharmacokinetic study of triapine, a potent ribonucleotide reductase inhibitor, administered daily for five days in patients with advanced solid tumors. Clin. Cancer Res. 9, 4092–4100.
Nejabatdoust, A., Salehzadeh, A., Zamani, H., et al., 2019. Synthesis, characterization and functionalization of ZnO nanoparticles by Glutamic Acid (Glu) and conjugation of ZnO@Glu by thiosemicarbazide and its synergistic activity with ciprofloxacin against multi-drug resistant Staphylococcus aureus. J. Clust. Sci. 30, 329–336.
Pape, V.F.S., Tóth, S., Füredi, A., Szebényi, K., Lovrics, A., Szabó, P., Wiese, M., Szakács, G., 2016. Design, synthesis and biological evaluation of thiosemicarbazones, hydrazinobenzothiazoles and arylhydrazones as anticancer agents with a potential to overcome multidrug resistance. Eur. J. Med. Chem. 117, 335–354.
Peña-Morán, O.A., Villarreal, M.L., Álvarez-Berber, L., Meneses-Acosta, A., Rodríguez-López, V., 2016. Cytotoxicity, post-treatment recovery, and selectivity analysis of naturally occurring podophyllotoxins from Bursera fagaroides var. fagaroides on breast cancer cell lines. Molecules. 21 (8), 1013.
Pingaew, R., Prachayasittikul, S., Ruchirawat, S., Prachayasittikul, V., 2013. Synthesis and cytotoxicity of novel N-sulfonyl-1,2,3,4tetrahydroisoquinoline thiosemicarbazone derivatives. Med. Chem. Res. 22 (1), 267–277.
Qi, J., Qian, K., Tian, L., Cheng, Z., Wang, Y., 2018. Gallium(III)–2-benzoylpyridine-thiosemicarbazone complexes promote apoptosis through Ca2+ signaling and ROS-mediated mitochondrial pathways. New J. Chem. 42, 10226–10233.
Redza-Dutordoira, M., Averill-Bates, D.A., 2016. Activation of apoptosis signalling pathways by reactive oxygen species. Biochim. Biophys. Acta. 1863, 2977–2992.
Richardson, D.R., Kalinowski, D.S., Richardson, V., Sharpe, P.C., Lovejoy, D.B., Islam, M., Bernhardt, P.V., 2009. 2-Acetylpyridine thiosemicarbazones are potent iron chelators and antiproliferative agents: Redox activity, iron complexation and characterization of their antitumor activity. J. Med. Chem. 52 (5), 1459–1470.
Saudi Moh, 2013. Health awareness center: "Cancer incidence in the Kingdom, compared to the global incidence, Is still low. https://www.moh.gov.sa/en/Ministry/MediaCenter/News/Pages/news-2013-02-04-002.aspx (accessed 2May 2021).
Shahrokhshahi, A., Salehzadeh, A., Vaziri, H.R., Moradi-Shoeili, Z., 2021. The Co(OH)2@Glu-TSC nanoflakes enhance the apoptosis in hepatoma G2 cell. J. Chinese Chem. Soc. 68 (8), 1574–1585.
Silva, T.D.d-S, Bomfim, L.M., Ana Carolina Borges da Cruz Rodrigue, A.C.B.da-C., Dias, R.B., Sales, C.B.S., Rocha, C.A.G., Soares, M.B.P., Bezerra, D.P., Cardoso, M.V.de-O, Leite, A.C.L., Militão, G.C.G., 2017. Anti-liver cancer activity in vitro and in vivo induced by 2-pyridyl 2,3-thiazole derivatives. Toxicol. Appl. Pharmacol. 329, 212–223.
Song, J., Pan, R., Li, G., Su, W., Song, X., Li, J., Liu, S., 2020. Synthesis and anticancer activities of thiosemicarbazones derivatives of thiochromanones and related scaffolds. Med. Chem. Res. 29, 630–642.
Wang, Y., Gu, W., Shan, Y., Liu, F., Xu, X., Yang, Y., Zhang, Q., Zhang, Y., Kuang, H., Wang, Z., Wang, S., 2017. Design, synthesis and anticancer activity of novel nopinone-based thiosemicarbazone derivatives. Bioorg. Med. Chem. Lett. 27, 2360–2363.
Yang, F., Liang, H., 2018. Designing anticancer multitarget metal thiosemicarbazone prodrug based on the nature of binding sites of human serum albumin carrier. Future Med. Chem. 10, 1881–1883.
Yee, E.M.H., Brandl, M.B., Black, D.S., Vittorio, O., Kumar, N., 2017. Synthesis of isoflavene-thiosemicarbazone hybrids and evaluation of their anti-tumor activity. Bioorg. Med. Chem. Lett. 27 (11), 2454–2458.
Yousef, T.A., Badria, F.A., Ghazy, S.E., El-Gammal, O.A., Abu El-Reash, G.M., 2011. In vitro and In vivo antitumor activity of some synthesized 4-(2-pyridyl)-3-Thiosemicarbazides derivatives. Int. J. Med. Med. Sci. 3 (2), 37–46.
Ziegler, D.S., Kung, A.L., 2008. Therapeutic targeting of apoptosis pathways in cancer. Curr. Opin. Oncol. 20, 97–103.